Purdue University
Purdue e-Pubs

International Compressor Engineering Conference   School of Mechanical Engineering

2012

Calculated Optimal Mechanical Efficiency of a Large Capacity Reciprocating Compressor

Takuma Tsuji
d10201@oecu.jp

Tatsuya Oku

Noriaki Ishii

Keiko Anami

Charles W. Knisely

Follow this and additional works at: http://docs.lib.purdue.edu/icec

Calculated Optimal Mechanical Efficiency of
a Large Capacity Reciprocating Compressor

Takuma TSUJI[1], Tatsuya OKU[2], Noriaki ISHII[1], Keiko ANAMI[3]
Charles W. KNISELY[4], Takashi MAEDA[1], Atsushi YAMAMOTO[2]

[1]Osaka Electro-Communication Univ.,
Dept. of Mechanical Engineering, Osaka, Japan.
Tel/Fax: +81-72-820-4561, E-mail: ishii@isc.osakac.ac.jp
[2]Mayekawa MFG. Co., Ltd., Ibaragi, Japan,
Tel: +81-297-48-1364, Tel/Fax: +81-284-62-0605, E-mail: tatsuya-oku@mayekawa.co.jp
[3]Ashikaga Institute of Technology, Dept. of Mechanical Engineering,
Tochigi, Japan.
Tel: +81-284-62-0605, E-mail: anami@ashitech.ac.jp
[4]Bucknell Univ., Dept. of Mechanical Engineering,
Lewisburg, Pennsylvania, USA
Tel: 570-577-1817, Fax: 570-577-7281, E-mail: knisely@bucknell.edu

ABSTRACT

In this study, calculations of the mechanical efficiency of a large reciprocating compressor, developed by Mayekawa MFG. Co., Ltd., with a per cylinder suction volume of 1300 cm^3 were carried out. These calculations were used to confirm whether the empirical combination of major design parameters in the Mayekawa compressor delivers optimal mechanical efficiency. Initially, the theoretical equation of motion of the rotating crankshaft is developed. Subsequently, computer calculations are carried out to determine the mechanical efficiency for various combinations of the major design parameters for operating speeds of 800, 1000 and 1200 rpm. From these calculations, the optimal combination parameters yielding the maximum mechanical efficiency could be determined, and then compared with the empirical combination used in the Mayekawa compressor.

1. INTRODUCTION

While optimal design guidelines have been developed and documented for scroll and rolling-piston rotary refrigerant compressors (see references [1-14] for scroll compressors, and references [15-20] for rolling-piston-rotary compressors), such design guidelines for the maximum performance of reciprocating compressors, on the other hand, are substantially less developed, even though the reciprocating compressor was among the earliest classical compression devices. Most dynamic analyses for the reciprocating compressor, such as references [2l-26], have focused on vibration characteristics. The equation of motion of the rotating crankshaft and the inertia forces exciting vibration of the whole compressor were derived to calculate mechanical vibrations of a compact refrigerant compressor, synchronized with the crankshaft rotation [21, 22]. Subsequently, higher frequency vibrations of the whole compressor, caused by elastic vibrations of the crankshaft, were experimentally identified and simulated in numerical studies [23, 24]. Finally, higher frequency vibrations of reed valves have been identified in experiments, and criteria for the onset of vibration and the volumetric similarity between reciprocating compressors and rolling-piston-rotary compressors have been developed [25-26].

Despite the relatively recent development and manufacturing of scroll compressors and rolling-piston-rotary compressors for use with refrigerants in cooling appliances in the early 1980s in Japan, optimal design guidelines for these compressors are more extensively developed. Indeed, the optimal design of these compressors was a major focus of the authors' research since their introduction. As a starting point, the equations of motion of compressor moving elements were derived to identify the constraint forces at each pair of compressor elements, ultimately permitting analysis in terms of the equation of motion of the rotating crankshaft. Further, the inertia forces exciting the vibration of the compressor body were derived and used to calculate the mechanical vibrations of the compressor, which are basically synchronized with the crankshaft rotation. Subsequently the mechanical, volumetric and overall compression efficiencies have been calculated, where the frictional losses, the compressed-gas leakage losses and the heat losses are all taken into consideration. As a result, optimal design guidelines for maximum efficiency have been established for scroll compressors [1-14] and for rolling-piston-rotary compressors [15- 20].
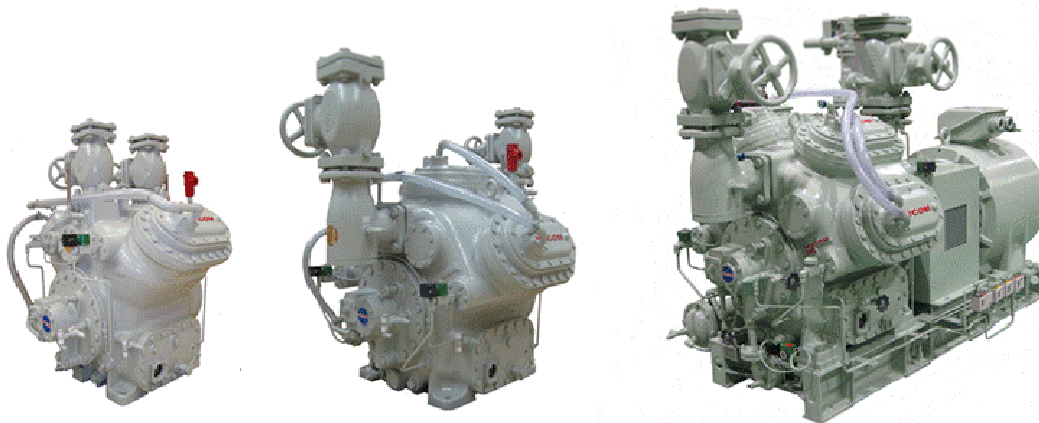
(a) 4-cylinder model 4WBHE   (b) 6-cylinder model 6WBHE   (c) 8-cylinder model 8WBHE
Figure 1: Reciprocating compressors in the WBHE series developed by Mayekawa MFG. Co., Ltd.

The authors' research on optimal design guidelines for scroll compressors and rolling-piston-rotary compressors were all based on an early optimal design concept for reciprocating compressors. About 30 years ago, the authors' interest was diverted from reciprocating compressors to scroll and rotary compressors due to the intense market demand. With the authors' focus on scroll and rotary compressors, the further development of optimal design guidelines for reciprocating compressors was delayed. Now with renewed commercial interest in reciprocating compressors for domestic refrigerators and for large capacity refrigeration units, it is appropriate for us to revitalize our study the optimization of reciprocating compressors.

For reciprocating compressors, the constraint forces at each pair of compressor elements depend not only upon the compression pressure and the inertia forces, but also upon the combination of piston diameter and stroke for a given suction volume. The suction volume for a given reciprocating compressor is determined by the piston diameter and the stroke. Consequently, there are many combinations of piston diameter and stroke for a specified suction volume. The constraint forces and the frictional power loss at each element pair are also dependent upon the selected combination of major parameters, thereby resulting in a different mechanical efficiency. Thus, selection of the optimal combination of major parameters is necessary to fundamentally ensure the maximum mechanical efficiency for the reciprocating compressor. Currently, however, the optimization of reciprocating compressors is not well developed, and the selection of combinations of major parameters has been empirically based. Such low-level technology requires a focused program to develop rational design guidelines for optimal efficiency as soon as possible. Such rational design guidelines are absolutely necessary to facilitate further development of superior reciprocating compressor with the highest possible performance.

From this perspective, optimization of small cooling capacity reciprocating compressors for domestic refrigerators was studied by Tsuji, *et al.* [27, 28]. The present study focuses on a large cooling capacity reciprocating compressor with the per cylinder suction volume of 1300 cm^3, which was developed for commercial market by Mayekawa MFG. Co., Ltd.. Figure 1 shows the four, six and eight-cylinder models in their commercial WBHE series. The piston diameter and stroke were empirically determined to be 130 mm and 100 mm, respectively. The intent of the present study is to determine whether this empirical selection of piston diameter and stroke yield a machine with optimal mechanical efficiency.

First, the theoretical development of the equations of motion for the crankshaft rotation and expressions for the constraint forces at all pairs of compressor elements are summarized. Then the energy equation for reciprocating compressors is derived. Subsequently, detailed example calculations of the mechanical efficiency, along with the crankshaft speed fluctuation ratio, are presented for the reciprocating compressor with a per cylinder suction volume of 1327 cm^3, driven by an induction motor at a crankshaft speed of 1000 rpm. Calculations were undertaken for various combinations of piston diameter and stroke, assuming coefficients of friction. From these calculations, the optimal combination that produces maximum mechanical efficiency could be identified. Finally, similar calculations were undertaken for crankshaft speeds of 800 and 1200 rpm, in order to examine the influence of the operating speed upon the optimization of the piston diameter and the piston stroke.

2. THEORETICAL DEVELOPMENT

A concentrated mass model of the piston-crank mechanism is presented in Figure 2(a), where the Cartesian coordinates (*x-y-z*) are introduced with the *z*-axis along the crankshaft center, the *x*-axis in the direction of the reciprocating piston motion and the *y*-axis perpendicular to the *x-z* plane. The crankshaft rotation angle a significant parameter, is given by θ relative to the *z*-axis, and the connecting-rod rotation angle, another parameter, is given by ϕ. The piston displacement from the crankshaft center is represented by x_p. As shown in Figure 2(b), the crankshaft, loaded by the gas force *P* on the piston, is driven by motor torque M_D, resulting in the constraint forces and frictional torques represented by Q_x, Q_y and M_Q at the crankshaft, S_x, S_y and M_S at the crank pin, and T_x, T_y and M_T at the piston pin, in addition to the frictional force *f* on the piston side wall.

The equations of motion for each of the moving machine elements shown in Figure 2(b) can be derived: one for the piston reciprocating in the *x*-axis, three for the connecting-rod moving in *x* and *y* directions and rotating with ϕ, and two for the crank arm moving in *x* and *y* directions, in addition to the main parameter, the crankshaft rotation θ. From the first six equations of motion, six constraint forces can be derived in terms of inertia forces, along with the gas force, the frictional force on the piston side wall and the frictional moments at the crank pin and piston pin. Substituting the derived constraint forces into the last equation of motion for the rotating crankshaft, the equation of motion of the crankshaft rotation can be reduced to the following expression:

$$I'_0\ddot{\theta} + (-m'_p\ddot{x}_p)x_p\tan\phi + \alpha\frac{\cos\theta}{\cos\phi}I'_c\ddot{\phi} = M_D - Px_p\tan\phi - \left\{ fx_p\tan\phi + \alpha\frac{\cos\theta}{\cos\phi}M_T + \frac{x_p}{l\cos\phi}M_S + M_Q \right\} \quad (1)$$

The terms on the left-hand side represent the inertia torques, where the first term is for the rotating crankshaft with a modified moment of inertia I_0', the second is for the reciprocating piston with a modified mass m_p' and the third is for the rotating connecting-rod with a modified moment of inertia I_c'. On the right-hand side, the first term is the supplied motor torque M_D, and the second through sixth terms are the load torques: the second due to gas force *P* on the piston, the third due to frictional force *f* on the piston side wall and the fourth through sixth due to the frictional torques M_T, M_S and M_Q. The length ratio of the crank arm to the connecting-rod is denoted by α.

The energy equation for the compressor can be derived by multiplying Equation (1) by a small angular displacement $d\theta$ and integrating each term over one revolution of the crankshaft. The energy supplied by the motor, E_s, goes primarily into the gas compression energy E_p and secondarily to overcome the friction losses E_f at the cylinder wall, E_{MT} at the piston pin, E_{MS} at the crank pin, and E_{MQ} at the crank journal:

$$E_s = E_p + E_f + E_{M_T} + E_{M_S} + E_{M_Q} \quad (2)$$

where

$$E_s = \int_{1rev.}M_D(\dot{\theta})d\theta, \qquad E_p = \int_{1rev.}P(\theta)x_p\tan\phi d\theta, \qquad E_f = \int_{1rev.}fx_p\tan\phi d\theta$$

$$E_{M_T} = \int_{1-rev.}\alpha\frac{\cos\theta}{\cos\phi}M_Td\theta, \qquad E_{M_S} = \int_{1-rev.}\frac{x_p}{l\cos\phi}M_Sd\theta, \qquad E_{M_Q} = \int_{1-rev.}M_Qd\theta \quad (3)$$

Where, motor torque is given in proportion to the crankshaft rotational speed $\dot{\theta}$.

Assuming Coulomb friction at each pair of elements, the friction forces can be derived by multiplying each resultant constraint force by each coefficient of friction, thus resulting in
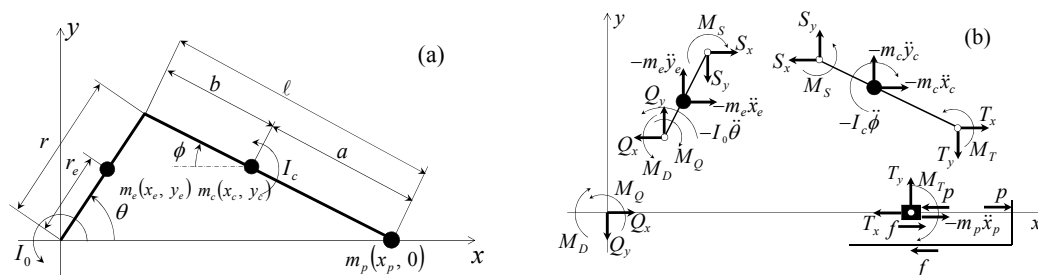

Figure 2: A representative model of piston-crank mechanism: (a) concentrated mass system and introduction of major constants and variables; (b) constraint forces, frictional forces and frictional moments at all pairs of machine elements.

$$f = \delta_2 \mu |T_y| \quad , \text{for TDC} < \theta < \text{BDC}: \delta_2 = +1, \text{ BDC} < \theta < \text{TDC}: \delta_2 = -1$$

$$M_T = \delta_3 \mu_T \sqrt{T_x^2 + T_y^2} \cdot r_T \quad \left(-\frac{\pi}{2} \leq \theta \leq \frac{\pi}{2} \rightarrow \delta_3 = +1, \quad \frac{\pi}{2} \leq \theta \leq \frac{3\pi}{2} \rightarrow \delta_3 = -1 \right)$$

$$M_S = \mu_S \sqrt{S_x^2 + S_y^2} \cdot r_S, \quad M_Q = \mu_Q \sqrt{Q_x^2 + Q_y^2} \cdot r_Q \tag{4}$$

where the coefficients of friction are represented by μ on the piston side wall, μ_T at the piston pin, μ_S at the crank pin, and μ_Q at the crank journal. Consequently, the energy equation, Equation (3), can be utilized to express the mechanical efficiency η_m as follows:

$$\eta_m = \frac{E_s - \left(E_f + E_{M_T} + E_{M_S} + E_{M_Q} \right)}{E_s} \tag{5}$$

3. CALCULATED RESULTS

3.1 Specifications for Calculation

Calculations were made for a large capacity reciprocating compressor for refrigerators with a suction volume of 1327 cm^3, and driven by an induction motor. The major specifications are listed in Table 1. The piston half-stroke r_0 and the piston diameter d_0 are 50 mm and 130 mm, respectively. The rated conditions of operation are 1000 rpm for the average speed, 0.098 MPa for the suction pressure P_s and 0.98 MPa for the discharge pressure P_d. The gas compression in the cylinder is assumed to be polytropic with an index n of 1.05. The coefficients of friction take a value of 0.083 on the cylinder wall, based on our previous experience, and 0.013 on the journal bearings at the crankshaft, crank pin and piston pin. The mechanical efficiency was

Table 1: Major specifications of
a reciprocating compressor for calculations

Volume of Cylinder	V_s	1327.0	[cm^3]
Average operation speed	N	1000	[rpm]
Piston diameter	d_O	130	[mm]
Mass of Piston	m_{p0}	2.65	[kg]
Mass of Connecting rod	m_{c0}	3.864	[kg]
Length of Connecting rod	L_0	300	[mm]
Conn-rod gravity from small end	a_0	299.9	[mm]
Conn-rod gravity from big end	b_0	0.0857	[mm]
Rotation radius of Crank pin	r_0	50	[mm]
Length ratio of Crank arm and Conn-rod		0.17	
coef. of friction between piston and cylinder	μ	0.083	
Coef. of friction of journal bearing	$\mu_{Q,S,T}$	0.013	
Suction pressure	P_s	0.098	[MPa]
Discharge pressure	P_d	0.98	[MPa]
Polytropic index	n	1.050	
Radius of Crank journal	r_Q	92	[mm]
Radius of Crank pin	r_S	90.00	[mm]
Radius of Piston pin	r_T	40	[mm]

calculated for a variety of combinations of the piston half-stroke r and the piston diameter d for the fixed suction volume of 1327 cm^3. The specific crank-arm-to-connecting-rod length ratio α was fixed at 0.17. According to the selected combination, the piston mass m_p, the connecting-rod mass m_c and its moment of inertia I_c may be adjusted in the following expressions:

$$m_p = \left(\frac{d}{d_0} \right)^2 m_{p0}, \quad m_c = \frac{l}{l_0} m_{c0}, \quad I_c = \left(\frac{l}{l_0} \right)^2 I_{c0} \tag{6}$$

In contrast, the moment of inertia of the crankshaft, I_0, does not need to be adjusted, since the motor power does not change meaningfully, for the fixed suction volume.

3.2 Dynamic behavior of rotating crankshaft

The equation of motion of the rotating crankshaft, given by Equation (1) can be numerically solved with an iterative calculation method. First, the 0th-order solution for the crank angle θ is calculated from Equation (1), assuming zero frictional force and moments. This 0th-order solution permits the calculation of friction forces and moments from Equations (4). Subsequently, these friction forces and moments are fed back into Equation (1), thus calculating the 2nd-order solution for θ. These iterative calculations continue until the solution for θ converges. Calculated results are shown in Figures 3(a) and 3(b), in which the rotational acceleration $\ddot{\theta}$ and the rotational velocity $\dot{\theta}$ are presented over one complete revolution of crank angle θ. In Figure 3(c), the velocity fluctuation ratio $\Delta\dot{\theta}/\dot{\theta}$ is presented for piston diameters d, ranging from 100 mm to 180 mm.

International Compressor Engineering Conference at Purdue, July 16-19, 2012
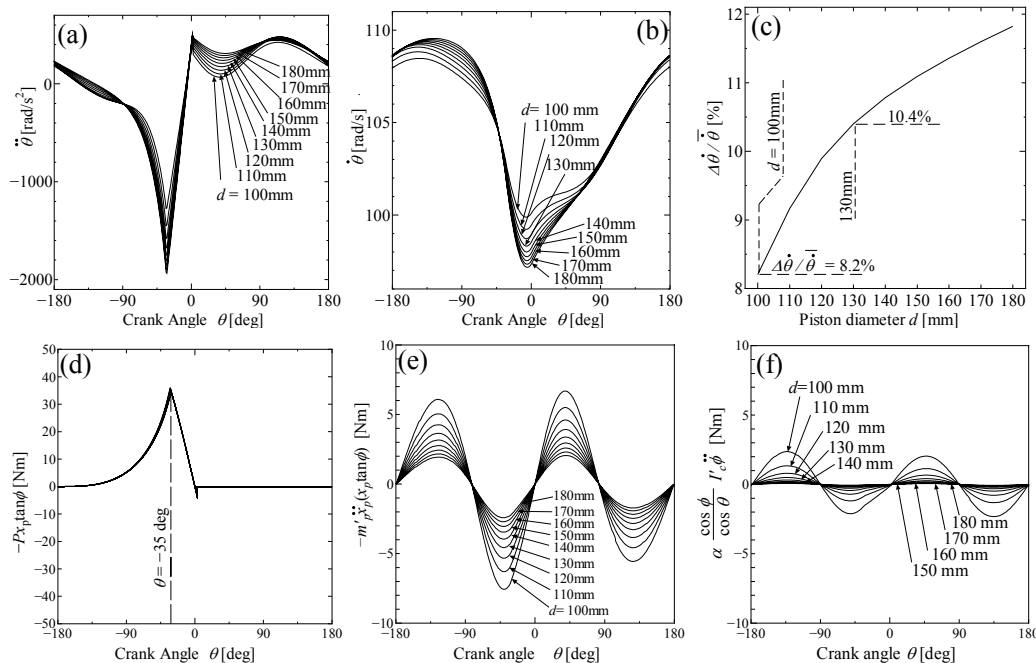
Figure 3: Calculated (a) rotational accelerations, (b) rotational velocity, (c) velocity fluctuation ratio, along with (d) gas compression force and inertia torques due to (e) the piston and (f) the connecting-rod torque for reciprocating compressors with V_S =1327 cm^3

At larger values of d, the acceleration exhibits a sharp negative peak at θ = -35°, which corresponds exactly to the sharp peak in gas compression torque curve, shown in Figure 3(d). Therefore, the gas compression is dominant over the acceleration. In contrast, however, at small d values, the negative peak in the acceleration curve decreases and the curve becomes a bit smoother, due to the increased piston inertia torque, shown in Figure 3(e), and the increased connecting-rod inertia torque shown in Figure 3(f). The piston inertia torque in Figure 3(f) reaches about -7.5 Nm at θ = -40°, while the gas compression torque in Figure 3(d) is naturally independent of d. Thus, the gas compression torque is increasingly canceled by the increasing piston and the connecting-rod torques as d decreases from 180 to 100 mm. The velocity fluctuation exhibits similar behaviors and, as shown in Figure 3(c), the velocity fluctuation ratio defined by $\Delta\dot\theta\left(\equiv \dot\theta_{max} - \dot\theta_{min}\right)/\overline{\dot\theta}$ also decreases with decreasing piston diameter d. The velocity fluctuation ratio reaches its minimum value of 8.2% at d =100 mm, while at d =130 mm the velocity fluctuation ratio is 10.4%.

3.2 Mechanical Efficiency

The friction force f and the friction torques M_T, M_S and M_Q can be calculated from Equations (4) as functions of the crank angle θ, and are plotted in Figure 4. The friction force f is determined by the side force on the cylinder, T_y, and hence the curves for large piston diameter d exhibit a sharp peak at θ = -35°, demonstrating the dominance of the gas force effect. On the other hand, the frictional torques M_T, M_S and M_Q exhibit a square form before reaching top dead center ($\theta = 0^o$), again indicative of the dominance of the gas force effect. As d decreases, the gas-force effect decreases and, in turn, the effect of inertia forces becomes dominant, as is clearly demonstrated in Figure 4(f) for f, in Figure 4(b) for M_S and in Figure 4(c) for M_Q. The inertia-force effect, while still present, is as great for M_T, shown in Figure 4(a), as for M_S and M_Q. These significant results regarding inertia-force effects are consistent with Equation (6), which shows the inertia forces of the connecting-rod, the mass m_c and moment of inertia I_c, all increase with decreasing d.

With the calculated results in Figures 3 and 4, the integrations given in Equation (3) can be carried out over one revolution of the crankshaft, resulting in the friction power losses, as shown in Figure 5(a). Three of the friction losses— E_{MS} at the crank pin, E_{MQ} at the crank journal and E_f at the piston wall—are relatively large, while E_{MT} at the piston pin is comparatively small. The friction losses E_{MS}, E_{MQ} and E_{MT} decrease with decreasing piston diameter d; and E_{MS} exhibits its minimum near d = 140 mm and then increases with a further decrease in d. In contrast, E_f increases gradually with decreasing piston diameter d. As a result, the net loss E_F due to friction
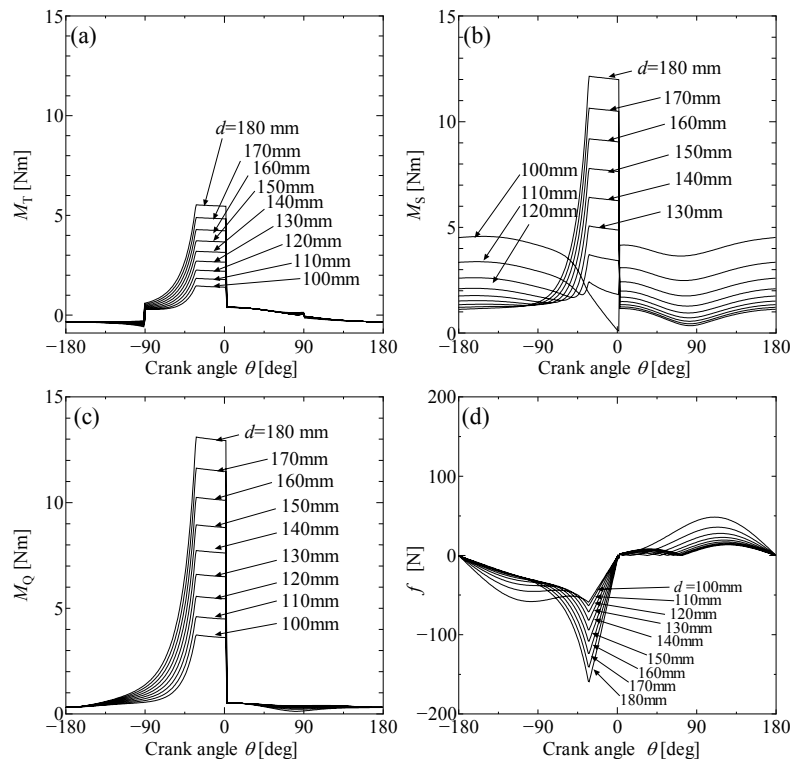
Figure 4: Friction torques at (a) the piston pin, (b) the crank pin, and (c) the crankshaft,
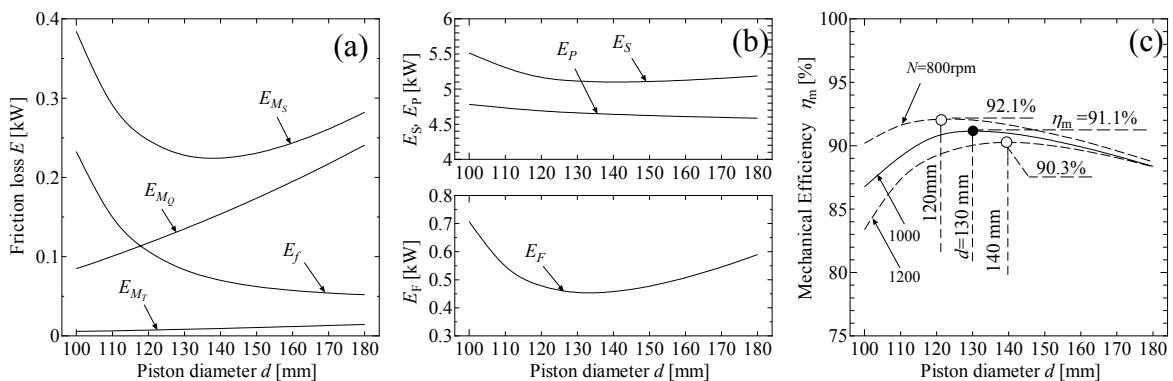and (d) friction force on the piston side wall.

Figure 5: Calculated (a) friction losses, (b) motor power, and (c) resulting mechanical efficiency for
reciprocating compressors with V_S =1327 cm^3.

exhibits a minimum at d =130 mm, as shown in Figure 5(b), in which the motor power E_S and the gas compression power E_P are also plotted.

Consequently, the mechanical efficiency η_m given by Equation (5) can be calculated and is plotted in Figure 5(c). As d decreases, η_m increases, exhibiting a maximum value of 91.1% at d =130 mm. The filled black circle at d = 130 mm represents the Mayekawa MFG. Co., Ltd. design, thus confirming that the empirically designed model is at the optimal point for an operating speed N of 1000 rpm.

Similar simulations were made for the other operating speeds of N = 800 and 1000 rpm, resulting in the dashed lines shown in Figure 5(c). When the operating speed is 800 rpm, the maximum mechanical efficiency occurs for a 120 mm piston diameter, plotted as the open circle in Figure 5(c), with a maximum value of 92.1%, 1% higher than for 1000 rpm. This result is because the inertia forces working at each of the pairs decrease with decreasing operating speed, thus shifting the optimal piston diameter d toward the smaller range 120 mm value. In contrast, when the operating speed increases to 1200 rpm, the influence of inertia is increases, shifting the
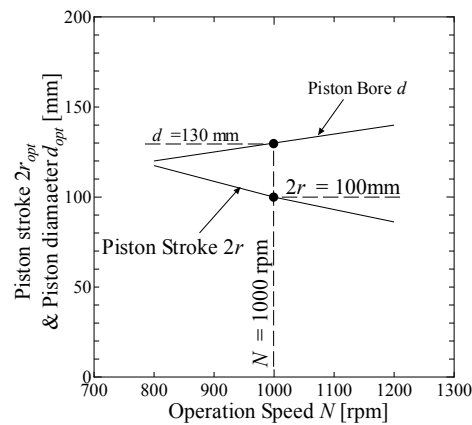
Figure 6: Optimal combination of piston diameter and piston stroke.

optimal piston diameter *d* toward a larger 140 mm value. The mechanical efficiency at 1200 rpm decreases by 0.8% relative to the value at 1000 rpm, taking on a value of 90.3 %.

The optimal combination of the piston diameter d_{opt} and stroke $2r_{opt}$ are shown in Figure 6, in which the abscissa is the operating speed *N*. With increasing operating speed, the optimal piston diameter increases linearly, while the piston stroke decreases also linearly. The design data by Mayekawa MFG. Co., Ltd. are plotted over the rated operating speed of 1000 rpm, where the piston diameter is 130 mm and the piston stroke is 100 mm, which exactly agree with the calculated optimal design values.

4. CONCLUSION

The optimal design of a 1300 cm^3 suction volume reciprocating compressor, developed by Mayekawa MFG. Co., Ltd. for commercial use in refrigerators, was carefully examined. The mechanical efficiency was calculated for various combinations of piston diameter and stroke at operating speeds of 800, 1000 (rated) and 1200 rpm. The optimal combinations of the piston diameter and stroke were determined.

The optimal design combination at the rated operating speed of 1000 rpm was a 130 mm piston diameter with a 100 mm piston stroke, yielding a maximum mechanical efficiency of 91.1%. It was a most pleasant surprise for the authors to find that the design values of piston diameter and piston stroke empirically determined by Mayekawa MFG. Co., Ltd., and precisely matched those found by the present theoretical optimization analysis.

NOMENCLATURE

a   : Length between gravity center of connecting-rod and small end center, m
a_0 : Basis of length between gravity center of connecting-rod and small end center, m
b   : Length between gravity center of connecting-rod and big end center, m
b_0 : Basis of length between gravity center of connecting-rod and big end center, m
d   : Piston diameter, m
d_0 : Basis piston diameter, m
$d_{opt.}$: Optimal piston diameter, m
E_f : Energy consumed between cylinder wall, W
E_{MQ} : Energy consumed at crank journal, W
E_{MT} : Energy consumed at crank pin, W
E_{MS} : Energy consumed at piston pin, W
E_P : Energy consumed by compressed gas, W
E_S : Energy supplied by motor, W
f   : Friction force between piston and cylinder, N
I_0 : Moment of inertia of crankshaft, kgm^2
I'_0 : Modified moment of inertia of crankshaft,

kgm^2
I_c : Inertia moment of connecting-rod, kgm^2
I_{c0} : Modified Moment of inertia of connecting-rod, kgm^2
I'_c : Moment of inertia of connecting-rod and modified one, kg m^2
l   : Length of connecting-rod, m
l_0 : Basis of length of connecting-rod, m
m_c : Mass of connecting-rod, m
m_{c0} : Basis of mass of connecting-rod, kg
m_p : Mass of piston, kg
m_{p0} : Basis of mass of piston, kg
m'_p : Modified mass of piston, kg
M_Q : Friction torque at crank journal, Nm
M_S : Friction torque at crank pin, Nm
M_T : Friction torque at piston pin, Nm
M_D : Motor torque, Nm
P   : Gas force, N
p_d : Discharge pressure, Pa

p_s : Suction pressure, Pa
Q_x : Constraint force of x – axis direction at crank journal, N
Q_y : Constraint force of y – axis direction at crank journal, N
S_x : Constraint force of x – axis direction at crank pin, N
S_y : Constraint force of y – axis direction at crank pin, N
T_x : Constraint force of x – axis direction at piston pin, N
T_y : Constraint force of y – axis direction at piston pin, N
r : Rotating radius of crank pin, m
r_0 : Basis of rotating radius of crank pin, m
$r_{opt.}$: Optimal rotating radius of crank pin, m
r_Q : Radius of crank journal, m
r_S : Radius of crank pin, m
r_T : Radius of piston pin, m

V_S : Suction volume of cylinder, m^3
x_p : Piston displacement, m
α : Specific length ratio of crank arm to connecting- rod, -
θ : Rotating angle of crankshaft, rad
$\dot{\theta}$: Rotational speed of crankshaft, rad/s
$\dot{\theta}_{min}$: Minimum rotational speed of crankshaft, rad/s
$\dot{\theta}_{max}$: Maximum rotational speed of crankshaft, rad/s
$\bar{\dot{\theta}}$: Average rotational speed of crankshaft, rad/s
$\ddot{\theta}$: Rotational acceleration of crankshaft, rad/s^2
ϕ : Oscillation angle of connecting-rod, rad
ε : Non-dimensional off-set value, -
μ : Coefficient of friction at cylinder wall, -
μ_Q : Coefficient of friction at crank pin, -
μ_S : Coefficient of friction at crank pin, -
μ_T : Coefficient of frictions at piston pin, -

REFERENCES

1. Ishii, N., Fukushima, M., Sawai K., Sano, K., Imaichi, K., 1988, Dynamic Behavior of a Scroll Compressor (Dynamic Analysis), JSME Int. Journal, Ser. 3, pp. 58-67.
2. Ishii, N., Yamamura, M., Morokoshi, H., Fukushima, M., Yamamoto, S., Sakai, M., 1988, On the Superior Dynamic Behavior of a Variable Rotating Speed Scroll Compressor, *Proc. of Int. Comp. Engrg. Conf. at Purdue*, pp. 75-82.
3. Ishii, N., Yamamura, M., Morokoshi, H., Muramatsu, S., Sawai, K., Osaka, M., Yamamura, M., 1987, Mechanical Efficiency of Various Large Capacity Scroll Compressors, *Proc. of 17ᵗʰ Int. Congress of Refrigeration*, Wien Austria, pp. 468-474.
4. Ishii, N., Yamamura, M., Muramatsu, S., Yamamoto, S., Sakai, M., 1990, Mechanical Efficiency of a Variable Speed Scroll Compressor, *Proc. of Int. Comp. Engrg. Conf. at Purdue*, Vol.1, pp. 192-199.
5. Ishii, N., Yamamoto, S., Muramatsu, S., Yamamura, M., Takahashi, M., 1992, Optimum Combination of Parameters for High Mechanical Efficiency of a Scroll Compressor, *Proc. of Int. Comp. Engrg. Conf. at Purdue*, pp. 118a1-118a8.
6. Ishii, N., Yamamura, M., Muramatsu, S., Yamada, S., Takahashi, M., 1994, A Study on High Mechanical Efficiency of a Scroll Compressor with Fixed Cylinder Diameter, *Proc. of Int. Comp. Engrg. Conf. at Purdue*, Vol.2, pp. 677-682.
7. Ishii, N., Sakai, M., Sano, K., Yamamoto, S., Otokura, T., 1996, A Fundamental Optimum Design for High Mechanical and Volumetric Efficiency of Compact Scroll Compressors, *Proc. of Int. Comp. Engrg. Conf. at Purdue*, Vol. II, pp. 639-644.
8. Ishii, N., Yamamoto, S., Sano, K., Sawai, K., Hiwata, A., Nakamoto, T., Kawano, H., 2002, Efficiency Simulations of a Compact CO_2 Scroll Compressor and Its Comparison with Same Cooling Capacity R410A Scroll Compressor, *Proc. of Int. Comp. Engrg. Conf. at Purdue*, C22-2(CD-ROM).
9. Ishii, N., Kawamura, S., Yamamoto, S., Sawai, K., Hiwata, A., Nakamoto, T., Kawano, H., Ting, K S., 2002, Efficiency Simulations with Consideration of Heat Losses of R410 Compact Scroll Compressor for Its Optimal Performance, *Proc. of Int. Comp. Engrg. Conf. at Purdue*, C22-3(CD-ROM).
10. Oku, T., Ishii, N., Anami, K., Knisely, C.W., Sawai, K., Morimoto, T., Hiwata, A., 2008, Theoretical Model of Lubrication Mechanism in the Thrust Slide-Bearing of Scroll Compressors, HVAC&R Research Journal ASHRAE Vol.14, No.2, pp. 239-258.
11. Ishii, N., Oku, T., Anami, K., Knisely, C.W., Sawai, K., Morimoto, T., Iida, N., 2008, Experimental Study of the Lubrication Mechanism for Thrust Slide Bearings in Scroll Compressors, HVAC&R Research Journal ASHRAE Vol.14, No.3, pp. 453-465.
12. Ishii, N., Oku, T., Anami, K., Knisely, C.W., Sawai, K., Morimoto, T., Iida, N., 2008, Optimal Performance Design Guidelines of Thrust Slide-Bearing in Scroll Compressors for Maximum Efficiency, *Proc. of Int. Comp. Engrg. Conf. at Purdue*, 1428, pp. 1-8.
13. Ishii, N., Oku, T., Anami, K., Knisely, C.W., Sawai, K., Morimoto, T., Fujiuchi, K., 2008, Effects of Surface Roughness upon Gas Leakage Flow Through Small Clearances in CO_2 Scroll Compressors, *Proc. of Int. Comp. Engrg. Conf. at Purdue*, 1429, pp. 1-8.

14. Ishii, N., Oku, T., Anami, K., Knisely, C.W., Sawai, K., Morimoto, T., Iida, N., 2008, Optimal Performance Development of High-Pressure Type Ammonia Scroll Compressors for Maximum Efficiency, *Proc. of Int. Comp. Engrg. Conf. at Purdue*, 1425, pp. 1-8.
15. Imaichi, K., Fukushima, M., Muramatsu, S., Ishii, N., 1982, Vibration Analysis of Rotary Compressors, *Proc. of Int. Comp. Engrg. Conf. at Purdue*, pp. 275-282.
16. Ishii, N., Imaichi, K., Muramatsu, S., Fukushima, M., Matsunaga, H., 1984, The Study of Rolling Piston, Rotary Compressor Dynamic Behavior with Stopping to Reduce Noise and Vibration Level, *Proc. of Int. Comp. Engrg. Conf. at Purdue*, pp. 1-8.
17. Ishii, N., Fukushima, M., Yamamura, M., Muramatsu, S., Sano, K., Sakai, M., 1989, The High Mechanical Efficiency of Rolling–Piston Rotary Compressors, *Proc of the 2nd World Congress on Heating Ventilating, Refrigeration and Air Conditioning(CLIMA2000)*, Sarajevo, Yugoslavia, pp. 91-96.
18. Ishii, N., Fukushima, M., Yamamura, M., Fujiwara, S., Kakita, S., 1990, Optimum Combination of Dimensions for High Mechanical Efficiency of a Rolling–Piston Rotary Compressor, *Proc of Int. Comp. Engrg. Conf. at Purdue*, Vol. 1, pp. 418-424.
19. Ishii, N., Morita, N., Ono, M., Yamamoto, S., Sano, K., 2000, Net Efficiency Simulations of Compact Rotary Compressors for Its Optimal Performance, *Proc. of Int. Comp. Engrg. Conf. at Purdue*, Vol. I, pp. 475-482.
20. Ishii, N., Morita N., Kurimoto, M., Yamamoto, S., Sano K., 2000, Calculations for Compression Efficiency Caused by Heat Transfer in Compact Rotary Compressors, *Proc. of Int. Comp. Engrg. Conf. at Purdue*, Vol. I, pp. 467-474.
21. Ishii, N., Imaichi, K., Kagoroku, N., Imasu, K., 1975, Vibrations of a Small Reciprocating Compressor, Design Engng. Technical Conf., Washington D. C, ASME, pp. 1-12.
22. Imaichi, K., Ishii, N., Imasu, K., Murai, M., 1979, A Device for Stopping Single-Cylinder Reciprocating Compressors Silently by Greatly Reducing Vibrations, *Proc. of 15th Int. Congress of Refrigeration*, Vol. II, pp. 727-733.
23. Ishii, N., Imaichi, K., Muramatsu, S., Fukushima, M., 1983, A Computer Simulation of Higher Frequency Vibrations of A Reciprocating Compressors, *Proc. of 16th Int. Congress of Refrigeration*, pp. 418-423.
24. Imaichi, K., Ishii, N., Imasu, K., Muramatsu, S., Fukushima, M., 1984, A Vibration Source in Refrigerant Compressors, Transactions of the ASME, Journal of Vibration, Stress, Reliability and Design, Vol. 106, pp. 122-128.
25. Ishii, N., Fukuoka, H., Matsunaga, H., Fukushima, M., Nakazumi, K., 1993 Dynamic Stability Criterion for Reed Valves in Refrigerant Compressors, JSME Int. Journal, Ser C, Vol. 36, No.1, pp. 69-76.
26. Ishii, N., Hitotsubashi, M., Yamamoto, S., Matsunaga, H., Hashimoto, T., Sano K., 1998, Volumetric Similarity for Vibrations of Reed Valve in Refrigerant Compressors, *Proc. of Int. Comp. and Their Systems*, London, pp. 99-104.
27. Tsuji, T., Ishii, N., Oku, T., Anami, K., Sawai, K., Morimoto, T., Matsui, A., Knisely, C. W., 2009, Fundamental Optimal Design Guideline for Reciprocating Compressors to Maximize Mechanical Efficiency, *Proc. of 7th International Conference on Compressors and Coolants Compressors 2009 (in CD-ROM)*, Papiernicka, Slovak Republic.
28. Tsuji, T., Ishii, N., Anami, K., Sawai, K., Hiwata, A., Morimoto, T., Sano, K., Knisely, C. W. Fundamental Optimal Performance Design Guidelines for Off-Set Type Reciprocating Compressors to Maximize Mechanical Efficiency, *Proc. of Int. Comp. Engrg. Conf. at Purdue*, 1358(in CD-ROM).

ACKNOWLEDGEMENTS